

TSC2 Loss in Lymphangioleiomyomatosis Cells Correlated with Expression of CD44v6, a Molecular Determinant of Metastasis

Gustavo Pacheco-Rodriguez,¹ Wendy K. Steagall,¹ Denise M. Crooks,¹ Linda A. Stevens,¹ Hiroshi Hashimoto,¹ Shaowei Li,² Ji-an Wang,² Thomas N. Darling,² and Joel Moss¹

¹Pulmonary-Critical Care Medicine Branch, National Heart, Lung, and Blood Institute, NIH and ²Department of Dermatology, Uniformed Services University of the Health Sciences, Bethesda, Maryland

Abstract

Lymphangioleiomyomatosis (LAM), a rare multisystem disease found primarily in women of childbearing age, is characterized by the proliferation of abnormal smooth muscle-like cells, LAM cells, that form nodules in the pulmonary interstitium. Proliferation of LAM cells results, in part, from dysfunction in tuberous sclerosis complex (TSC) genes *TSC1* (hamartin) and/or *TSC2* (tuberin). Identification of LAM cells in donor lungs, their isolation from blood, and their presence in urine, chylous ascites, and pleural effusions are consistent with their ability to metastasize. Here, we investigated the presence on LAM cells of the hyaluronic acid receptor CD44 and its splice variants associated with metastasis. The heterogeneous populations of cells grown from lungs of 12 LAM patients contain cells expressing mRNA for the variant CD44v6. Histologically, CD44v6 was present in LAM lung nodules, but not in normal vascular smooth muscle cells. CD44v6-positive sorted cells showed loss of heterozygosity at the *TSC2* locus; binding of CD44v6 antibody resulted in loss of cell viability. Levels of CD44 were higher in cultured Eker rat (*Tsc2*^{-/-}) cells than in *Tsc2*^{+/+} cells, but unlike human LAM cells, the *Tsc2*^{-/-} Eker rat cells did not contain CD44v6 splice variant mRNA. CD44 splicing and signaling is regulated by osteopontin. Plasma from LAM patients contained higher concentrations of osteopontin than plasma of healthy, age-, and sex-matched volunteers ($P = 0.00003$) and may be a biomarker for LAM. The cell surface receptor CD44 and its splice variant CD44v6 may contribute to the metastatic potential of LAM cells. [Cancer Res 2007;67(21):10573–81]

Introduction

Lymphangioleiomyomatosis (LAM), a rare multisystem disease found primarily in women of childbearing age, presents in a sporadic manner or in association with tuberous sclerosis complex (TSC), an inherited disorder. LAM is characterized by the aberrant proliferation of smooth muscle-like cells (LAM cells) that form nodules in the pulmonary interstitium (1, 2). In addition, LAM or LAM/TSC may be associated with renal angiomyolipomas and infiltration of the axial lymphatics. Patients presenting with TSC may exhibit typical skin lesions, including angiofibromas and periungual fibromas (3).

The LAM lesions in lungs of patients with sporadic presentation of the disease possess mutations in the *TSC2* gene, which encodes tuberin (4). TSC protein abnormalities in LAM may lead to dysregulation of the mammalian target of rapamycin, with increased p70 S6 kinase activity (5, 6). In addition to abnormalities in TSC, LAM cells within the nodular lung structures contain proteins that react with antibodies against the Pmel17 gene product, gp100 (HMB-45 immunoreactivity) and MART-1 (1, 7). The LAM cells also exhibit a smooth muscle phenotype and contain immunoreactive smooth muscle actin (SMA). The relationship of the smooth muscle-like and melanocytic phenotypes to mutations in the *TSC* genes is not clear.

The multisystem manifestations of LAM have been correlated with a metastatic dissemination of the LAM cells (4, 8, 9), which were identified in donor lungs transplanted to LAM patients (10, 11). Furthermore, LAM cells have been detected in blood, chyle, and urine (8). Thus, metastasis seems to be a mechanism by which LAM cells are disseminated but the molecular determinants are unknown.

CD44 is a class I transmembrane glycoprotein encoded by 21 exons present in chromosome 11, and specific splice isoforms of this molecule have been identified as molecular determinants of metastasis (12–14). The standard form (CD44s) encoded by exons 1 to 5 and 6 to 10 is found ubiquitously with a predicted molecular weight of ~37 kDa; however, the proteins identified by monoclonal antibodies range in size from 80 to 200 kDa due to glycosylation variants. The production of CD44 splice isoforms are regulated mainly by signaling mechanisms involving the Ras-mitogen-activated protein kinase pathway (12, 15). Isoforms generated by splicing using the 10 additional exons v1 to v10 result in an insertion of a segment within the extracellular portion of the molecule.

The CD44 extracellular domain is responsible for binding of hyaluronic acid, E-selectin, osteopontin, hepatocyte growth factor, and Fas ligand (12, 16, 17). In addition, the extracellular domain of CD44 binds metalloproteases, including MMP7 and MMP9, which cleave CD44s as well as variant 6 (CD44v6; ref. 18). CD44v6 has been associated with tumorigenicity and is involved in homing during metastasis (13).

CD44 splicing is regulated, in part, by growth factors such as osteopontin and hepatocyte growth factor (19, 20). Osteopontin is chemokine-like molecule with multiple domains including an arginine-glycine-aspartate (RGD) domain, which promotes binding to integrins, and a CD44-binding domain. It also contains a thrombin cleavage site and can be a substrate for MMP7 (21, 22). Multiple cell types, including smooth muscle cells, express this adhesive glycoprotein. Interestingly, osteopontin binds CD44v6 and CD44v3 (23, 24). Thus, CD44 and its splice variants are involved in multiple cellular processes required for metastasis, and osteopontin seems to be one of the main regulators of CD44 function and splicing. Lungs are common sites of metastases for breast cancer

Note: Supplementary data for this article are available at Cancer Research Online (<http://cancerres.aacrjournals.org/>).

Requests for reprints: Gustavo Pacheco-Rodriguez, Pulmonary-Critical Care Medicine Branch, National Heart, Lung, and Blood Institute, NIH, Building 10/Room 5N307, 9000 Rockville Pike, Bethesda, MD 20892-1434. Phone: 301-594-5705; Fax: 301-402-1610; E-mail: pachecog@nhlbi.nih.gov.

©2007 American Association for Cancer Research.
doi:10.1158/0008-5472.CAN-07-1356

and melanoma among other malignancies (25, 26), in which the hyaluronic acid receptor CD44 plays a role (12). The splice variant CD44v6 has been associated with and was shown to function in multiple metastatic tumors (27). Because LAM cells seem to have metastatic potential, we asked whether CD44 and its splice variants are expressed in LAM cells. The variant CD44v6 was detected on cultured LAM cells from explanted lung with loss of heterozygosity (LOH) for *TSC2*. LAM cells within the lung nodules, but not normal vascular cells, expressed CD44v6 on the exterior surface, which may contribute to their metastatic potential and be a potential therapeutic target.

Materials and Methods

Patient population. The study group comprised patients (age 34–54 years) in whom the diagnosis of LAM was made on the basis of clinical, radiologic, and histopathologic findings. Tissue was obtained at the time of lung transplantation or elective skin biopsy. The patients consented under a protocol (95-H-0186) approved by the National Heart, Lung, and Blood Institutional Review Board.

Isolation of cells from LAM lung. To culture cells from explanted lungs of LAM patients, lung sections (1–3 mm) obtained at the time of transplant were placed on plastic dishes. Cells were grown in mesenchymal cell culture medium (Cambrex) for ~1 week. Mesenchymal cell medium contains 0.05 unit/mL of penicillin, 0.05 µg/mL of streptomycin, and 4 mmol/L glutamine supplemented with 10% fetal bovine serum, which promotes the growth of mesenchymal stem cells as determined by the potential of the grown cells to differentiate to adipocytes, chondrocytes, and osteoclasts (28). When small colonies of cells were formed, the tissue sections were removed and the cells were allowed to grow for 3 to 7 days before trypsinization and transfer to new plastic dishes. This procedure seems to select a mixture of cells that include those with LOH for *TSC2*.

Fluorescent *in situ* hybridization. Cells grown in LabTekII chambers were washed with Dulbecco's PBS (DPBS) containing 1 mmol/L CaCl₂ and 1 mmol/L MgCl₂. Cells were fixed in methanol/glacial acetic acid (3:1) at –20°C and incubated for 30 min at –20°C. Slides were air dried and stored at –20°C until use. A 199-kb BAC clone encompassing the *TSC1* gene (RP11-295G24) was purchased from Research Genetics and CDEB9, a 32-kb cosmid clone spanning the 5' untranslated region through exon 13 of the *TSC2* gene, was generously provided by Dr. David Kwiatkowski (Brigham and Women's Hospital, Boston, MA). Probes were labeled directly using Spectrum Green (*TSC1*) or Spectrum Orange (*TSC2*; Vysis). Nuclei were stained with 4',6-diamidino-2-phenylindole (DAPI). Images obtained using a BX40 fluorescence microscope (Olympus) fitted with an Orca ER digital charge-coupled device camera (Hamamatsu) were merged and analyzed using OPENLAB 3.0 software (Improvision). On average, ~20% of cells from initial cultures showed allelic deletion for *TSC2*.

Immunohistochemistry. Immediately after removal of lung tissue at lung transplantation or biopsy, thin slices were cut and fixed by immersion in buffered 10% formalin. The tissue sections of LAM lungs were from 10 women (age range 34–54 years), in whom the diagnosis of LAM was made on the basis of clinical, radiologic, and histopathologic findings. Lung tissues were from one biopsy at the time of the patient's initial diagnostic evaluation, in eight patients from explanted lung, and in one patient at autopsy. The tissues were dehydrated, embedded in paraffin, and sectioned to a thickness of 5 µm. To evaluate the localization and amount of immunoreactive CD44 and CD44v6, sections were immunostained by the peroxidase method (EnVision System; DAKO) using mouse monoclonal antibody against CD44 (G44-26; BD Biosciences; 1:200) and rabbit polyclonal antibodies against CD44v6 (EMD Biosciences; 1:200). Before staining for CD44, the sections were heated in an antigen-retrieval solution (Target Retrieval Solution; DAKO) in a microwave oven for 10 min, and cooled in the solution for 30 min.

To inactivate endogenous peroxidase activity, tissue sections were incubated with 2% H₂O₂ in methanol for 30 min at room temperature, then washed in PBS. Nonspecific binding of secondary antibody was

blocked by incubation with 5% normal horse or goat serum for 30 min, before sections were incubated with appropriate primary antibodies overnight at 4°C. After three washes with PBS, the peroxidase-labeled polymer from the EnVision System kit was applied for 1 h at room temperature, followed by washing with PBS, and color development with the 3,3'-diaminobenzidine substrate kit (Vector Laboratories). Sections were counterstained with Meyer's hematoxylin. Immunostaining with HMB-45 and anti-SMA antibodies identified LAM cells. Immunohistochemical control procedures included omission of the primary antibody and its replacement by appropriate concentrations of normal rabbit or mouse IgG. These controls were consistently negative. In addition, LAM cells were compared with other cells in histologically normal lung.

Dual staining for CD44v6 and gp100. Immunofluorescence with dual staining and laser scanning confocal fluorescence microscopy were used to evaluate colocalization of immunoreactivity for CD44v6 and gp100. Before staining with CD44v6 antibodies and HMB45, which reacts with gp100, sections were treated with 0.04% pepsin in 0.01 mol/L HCl for 15 min at 37°C and washed in PBS. The sections were incubated overnight at 4°C with a mixture of the two primary antibodies (diluted 1:20 and 1:10, respectively), and then for 1 h with FITC-labeled horse antibody against mouse IgG (1:100) and Texas red-labeled goat antibody against rabbit IgG (1:100; Vector Laboratories). After washing with PBS, sections were incubated with DAPI (Sigma Chemical) for 15 min and inspected with a confocal microscope (model TCS4D/DMIRBE; Leica), equipped with argon and argon-krypton laser sources.

Immunostaining of cultured cells. Cells grown as described were transferred to LabTek II slides, incubated overnight, and washed with PBS containing 1 mmol/L each of CaCl₂ and MgCl₂. Then, cells were fixed with 4% paraformaldehyde (Electron Microscopy, Inc.) and permeabilized with 0.1% Triton X-100 for 4 min at room temperature, followed by incubation with DPBS containing 3% bovine serum albumin and 5% goat serum for 1 h at room temperature. Cells were washed with DPBS, incubated with the indicated antibody at 4°C for ~12 h, washed again with DPBS, and incubated with secondary antibodies labeled with the indicated fluorophore for 1 h at room temperature. After washing, the slides were covered with Vectashield (Vector Laboratories) with or without DAPI and sealed with a coverslip.

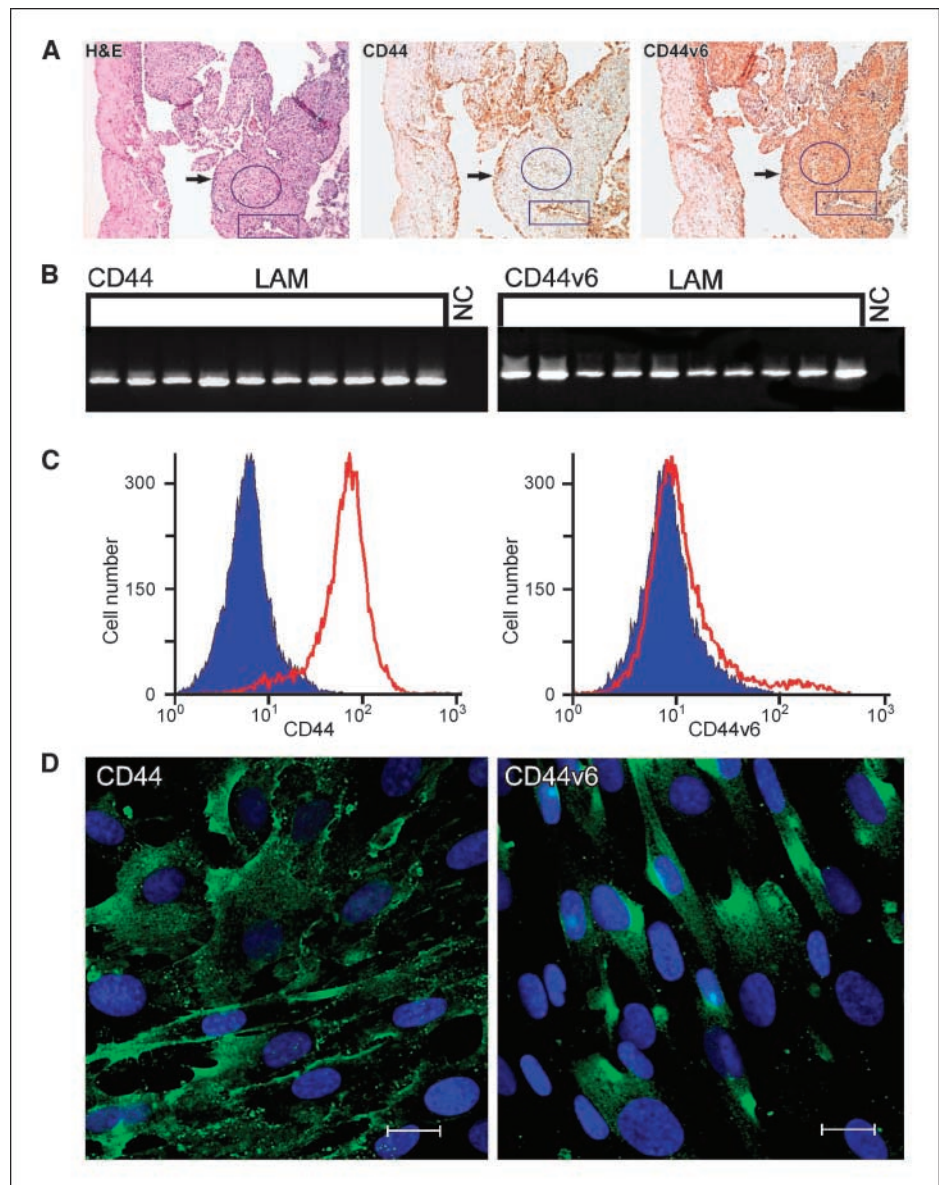
Quantitative analysis of cell fluorescence by confocal microscopy. Quantitative data images were acquired using identical settings of the instrument that avoid saturation of the brightest pixels. Series of 12-bit images along the z-axis were obtained throughout the cells with a ×40, 1.3-numerical-aperture Plan-Apochromat oil immersion objective. Analysis was done using Imaris 5.0.2. software package (Bitplane AG). The integrated sum of total fluorescence through all optical sections in the three-dimensional series is calculated and compared between EEF^{-/-} and EEF^{+/+} cells.

Reverse transcription-PCR of CD44 mRNA. mRNA was extracted from cells using the RNeasy mini kit from Qiagen; cDNA was prepared with the Superscript First Strand Synthesis System for reverse transcription-PCR (RT-PCR; Invitrogen); and PCR was done using primers described by Hudson et al. (29). As controls, PCR was done with actin- and/or glyceraldehyde-3-phosphate dehydrogenase-specific primers (Biosource International).

Fluorescence-activated cell sorting. Confluent cells in 100-mm dishes were washed with 10 mL PBS without calcium and magnesium and incubated with 1 mL 25 mmol/L EDTA and 0.25% trypsin. When cell detachment was observed microscopically, 10 mL of complete medium were added. Cells (~2 × 10⁶) collected by centrifugation at 500 × g were washed once with 10 mL DPBS, suspended in DPBS, and incubated for 30 min at room temperature with antibodies CD44-R-phycoerythrin (clone F10-44-2, Biosource International) and CD44v6-fluorescein (clone VFF-7, Biosource International) for human cells. Anti-CD44-fluorescein (clone OX-49) was used to detect expression of CD44 in rat cells, and anti-human CD9 (clone MM2/57) labeled with either RPE or fluorescein was also used to help in the identification of LAM cells.

7-Amino-actinomycin D (7AAD) was used to assess cell viability. Cell sorting was done on a MoFlo flow Cytometer (DakoCytomation, Inc.). Excitation light sources were 100 mW from an argon laser tuned to 488 nm

Figure 1. Immunoreactivity of LAM nodules to monoclonal antibodies against CD44 standard and CD44v6. **A**, H&E staining of an explanted LAM lung section showing the proliferative LAM cells (*oval*). *Arrow*, type II pneumocytes. *Rectangle*, vascular structure. LAM cells reactive with monoclonal antibody against CD44s. Type II pneumocytes (*arrow*) and vascular cells react strongly (*rectangle*), whereas LAM cells (*oval*) and endothelial-like cells within the nodule react moderately. LAM cells reactive with monoclonal antibody against CD44v6. Both spindle-shaped and epithelioid LAM cells show a strong reaction in cytoplasm and membranes (*oval*). Endothelial-like cells within the nodule were negative (*arrow inside oval*). *Rectangle*, vascular structure. **B**, CD44 standard and CD44v6 forms are expressed in LAM cell lines. LAM lines 1 to 10 contain mRNA for CD44 standard (exons 1–5) and CD44v6 as shown by RT-PCR. CD44 was detected using primers p1 and p2 (29) as described in Materials and Methods. *NC*, negative control (minus reverse transcriptase). **C**, flow cytometric analysis of cultured LAM cells showing that ~90% are positive for CD44 (clone F10-44-2, *red*). Flow cytometric analysis of cultured LAM cells showing 8% to 20% of cells positive for CD44v6 (clone VFF-7, *red*). *Blue histogram*, isotype (negative) control. **D**, LAM cells reactive with antibody against CD44s, which seem to be largely associated with the plasma membrane. Reactive LAM cells with anti-CD44v6 antibody show reactivity with several cells at the plasma membrane but large amounts were present within the cytoplasm. See Supplementary Fig. S4 for immunoreactive negative controls. *Blue*, nuclear staining (DAPI). *Bar*, 20 μ m.



and 35 mW from a HeNe laser emitting at 633 nm. Fluorescence signals were collected using amplifiers that reported on a logarithmic scale; forward and side scatter signals were recorded on a linear scale. Sorting was done using the "purify 1" mode. Sheath pressure was 60 psi and the sample differential pressure was 0.4 psi or less. Data acquisition, analysis, and compensation were done using Summit software (DakoCytomation). All data were stored as listmode files.

PCR analysis of LOH. Genomic DNA was isolated from sorted cells using the Qiamp blood minikit (Qiagen) or from whole blood by using the PureGene kit (Gentra Systems). DNA was amplified specifically by using primers flanking microsatellite loci D16S521, Kg8, D16S663, D16S3024, D16S3395, and D16S291 on chromosome 16p13. Antisense primers were labeled with fluorescent dyes (6-FAM or HEX, Invitrogen). Primer sequences were obtained from the Genome Database.³ PCR was done in 12.5- μ L mixtures containing 10 mmol/L Tris-HCl (pH 8.3), 50 mmol/L KCl, 2.5 mmol/L MgCl₂, 25 μ mol/L of each deoxynucleoside triphosphate, 0.8 μ mol/L primer, and 0.5 units of AmpliTaq Gold (Applied Biosystems),

using a Bio-Rad Mycycler with initial denaturation at 95°C for 2 min, followed by 28 cycles of 95°C (45 s), 55°C (45 s), and 72°C (1 min). PCR products were analyzed on a 3100 Genetic Analyzer (Applied Biosystems). Quotient LOH (QLOH) was calculated by comparing the ratio of fluorescence intensity of each allele in putative LAM (L) cells to that in whole blood (N) from the same patient: (L1/L2)/(N1/N2), where L1 or N1 is the minor allele. L2 and N2 represent the other allele. QLOH values of 0.6 or less were scored as LOH but could also be considered allelic imbalance.

Osteopontin determination. Osteopontin was quantified by ELISA in plasma from LAM patients and normal volunteers using the Human Osteopontin Immunoassay kit from R&D Systems. Samples were taken from a one-time visit, and the patients were selected randomly.

Results

CD44 is expressed in LAM cells. A typical LAM nodule showing areas of proliferating abnormal smooth muscle cells surrounded by hyperplastic type II pneumocytes is shown in Fig. 1A. Whereas LAM cells within the nodule reacted moderately with anti-CD44 antibody, hyperplastic type II pneumocytes (*arrow*) and vascular

³ <http://www.gdb.org>

endothelial cells were strongly immunoreactive (*rectangle*), consistent with previous results (ref. 30; see also Supplementary Fig. S1). Thus, CD44 seems to be present in LAM cells and other cells as well as in lymphocytes (Supplementary Fig. S2). The splice variant CD44v6 is a determinant of metastasis (14), and this variant was detected in proliferating spindle-shaped LAM. Some of the cells reactive with HMB-45 also reacted with anti-CD44v6 (Supplementary Fig. S2). Thus, the proliferating LAM cells were immunoreactive to anti-CD44v6, and only some epithelioid cells immunoreactive for HMB-45 were positive for anti-CD44v6. To identify the lymphatic structures involved in LAM lesions, we used antibody D2-40 that reacts with lymphatic endothelium but not with vascular endothelium (31). The reactivity was specific as nonspecific IgG did not react with LAM cells and type II pneumocytes (Supplementary Figs. S1 and S2).

Cells cultured from LAM lungs contain CD44 and CD44v6 mRNA and are immunoreactive to antibodies. We used the cell mixtures to evaluate CD44 mRNA in the cultured cell populations with RT-PCR designed to detect exons 1 to 5, which are found in the standard form of CD44 and all its splice variants, and we found CD44 mRNA in cells from 10 different patients (Fig. 1B).

Because CD44 is on the cell surface, we immunostained nonpermeabilized LAM cells with the antibody raised against CD44 (clone F-10-44-2) and determined by fluorescence-activated cell sorting (FACS) that ~90% of the cells were immunoreactive (Fig. 1C). The presence of this protein on the surface was corroborated by confocal microscopy showing that immunoreactive CD44 was localized on the cell surface with some seen intracellularly (Fig. 1D).

Approximately 10% to 20% of the cells expressed CD44v6 by flow cytometry (Fig. 1C). The presence of CD44v6 on the cell surface was confirmed by confocal microscopy (Fig. 1D). It was observed that a large fraction of the immunoreactivity of cultured cells was present not only in the periphery of the cells but also intracellularly (Fig. 1D), suggesting that CD44v6 is present in similar manner as found on normal dermal fibroblasts (Supplementary Fig. S3). Although we cannot rule out a mislocalization of CD44v6 in LAM cells, as has been seen with polycystin-1 in cells with dysfunctional TSC2 (32), we have observed that most of the immunoreactivity with anti-CD44v6 is present intracellularly in cells grown from explanted lungs of LAM patients.

Characterization of cells from LAM patients. We evaluated the presence of CD44 in cells cultured from explanted lungs of 12 patients with sporadic LAM, as described in Materials and Methods. To identify the presence of LAM cells within the heterogeneous population of LAM lung-derived cells, we detected the presence of cells with immunoreactivity with anti-SMA and HMB-45 antibodies, and LOH for *TSC1* and *TSC2* assays by fluorescence *in situ* hybridization (FISH) and/or PCR procedures (Fig. 2 and shown below). SMA was present in stress fibers as shown in other smooth muscle cells, including pulmonary artery smooth muscle cells (Fig. 2A). Approximately 20% of the cells grown from LAM lung reacted with anti-SMA. The distribution of the stress fibers in LAM cells differed from that in pulmonary artery smooth muscle cells. LAM cultures also contained a small percentage of cells that reacted with monoclonal antibody HMB-45 (Fig. 2B). The distribution of HMB-45 immunoreactivity in premelanosomal structures throughout the LAM cells was different than that in melanoma cells (MALME-3M), in which it was more concentrated in cell periphery (Fig. 2B). Cell cultures contained

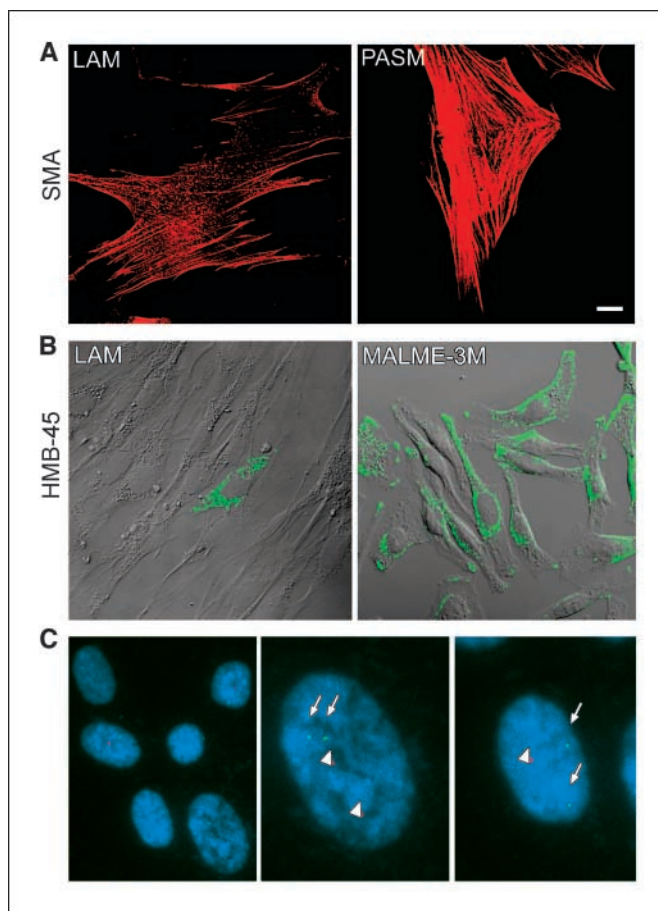


Figure 2. Characterization of LAM cell cultures. A, reaction of cells cultured from LAM lung and pulmonary artery smooth muscle cells (PASM) with monoclonal antibody against SMA. B, reaction of cultured LAM cells and MALME-3M with monoclonal antibody HMB-45. C, FISH for *TSC1* (green) and *TSC2* (red) in LAM cells showing normal presence of two of each allele as well as abnormal presence of *TSC2* alleles (left). FISH for *TSC1* (green, arrow) and *TSC2* (red, arrowhead) in LAM cell with one (right) or two *TSC2* (left) alleles. Bar, 20 μ m.

20% to 40% of cells lacking a *TSC2* allele as determined by FISH (Fig. 2C compare *right* and *left*). We were unable to detect large numbers of cells with alterations of *TSC1* nor did we detect loss of *TSC2* heterozygosity in these heterogeneous primary cell lines by PCR techniques (see below). The presence of reactive SMA antibodies and HMB-45, and the presence of cells with *TSC2* allelic deletion, are consistent with origination of these cells from LAM lung.

Cells cultured from lungs of LAM patients contain CD44v6mRNA and show LOH for *TSC2*. The presence of different CD44 splice variants was assessed in total RNA from 10 lines of cultured LAM cells. All cell lines tested contained mRNA for the splice variant CD44v6 (Fig. 1B; Supplementary Table S1), as well as for other variants. Because cells within LAM lung nodules reacted with anti-CD44v6 antibodies (Fig. 1), we were prompted to attempt separation of LAM cells based on that characteristic.

To define the relationship between LAM cells and CD44v6, we collected cells with immunoreactive CD44v6 in the surface by sorting (Fig. 3). Although the percentage of cells differed among patients, ~80% of the cells were CD44⁺CD44v6⁻, 5% to 15% CD44⁻CD44v6⁻, 5% to 10% CD44⁻CD44v6⁺, and 2% to 5%

CD44⁺CD44v6⁺ (e.g., Fig. 3B). DNA from sorted cells was extracted and tested for LOH of *TSC2* using microsatellite loci D16S521, D16S3395, Kg8, D16S663, and D16S291. We observed allelic imbalance that could represent LOH for *TSC2* in all the cells positive for CD44v6 (Table 1). Figure 3C shows two examples of LOH for *TSC2* in the separated cell populations. The top panel shows PCR products for the microsatellite repeat in the cell mixtures before separation in which no LOH was detected. Although we were not able to detect allelic imbalance or LOH regularly in cell mixtures, we were able to determine that a specific population separated with these antibodies exhibited abnormalities in the *TSC2* locus (see Fig. 3C, panels with the arrow). A summary of results for cell lines from 12 patients is shown in Table 1. The data on which our conclusions are based are summarized in Supplementary Table S2. Thus, cells immunoreactive for CD4v6 have abnormalities at the *TSC2* locus as evidenced by LOH for *TSC2*.

Cells immunoreactive with CD44v6 antibody are permeable to 7AAD. As binding of antibodies to CD44 has been correlated with cell death (17), we investigated the viability of cells after exposure to these antibodies using the cell-permeating dye 7AAD (33). Reaction of cells with either CD44 or CD44v6 antibodies increased the number of cells permeable to 7AAD (Fig. 3D). Among the ~20% of nonviable cells, 80% to 90% were those that reacted

with CD44v6, and only ~10% reacted with CD44, suggesting that reaction of LAM cells with anti-CD44v6 made them prone to cell death (Fig. 3D). Because the majority of the cells were dead after sorting, further studies were not possible.

Overexpression of CD44 correlated with loss of *Tsc2* in rat cells. To assess the presence of CD44 and CD44v6 in cells lacking *Tsc2*, we used a *Tsc2*^{-/-} (EEF^{-/-}) cell line from Eker rats (34) and a cell line derived from it that expresses a wild-type *Tsc2* gene, cell line EEF^{+/+} (*Tsc2*^{+/+}). By confocal immunofluorescence, we showed that there are 14.4 times (Fig. 4A, inset) more CD44 in *Tsc2*^{-/-} expressed than in *Tsc2*^{+/+}. The difference in fluorescence intensity was determined on two-dimensional projections (using maximum-pixel-intensity algorithm) of the three-dimensional fluorescence, generated and presented as merged FITC/DAPI channels. The FITC fluorescence intensities are color-coded using a look-up table with a 0 to 4,095 range to create pseudocolor-mapped images (Fig. 4A). FACS analysis and immunohistochemistry also showed a marked difference on the levels of CD44 expression (Fig. 4A and B). CD44 mRNA was present in *Tsc2*^{-/-} and *Tsc2*^{+/+} cells (Fig. 4C) but expression of CD44v6 mRNA was not detected in either cell line (Fig. 4C). CD44 was less abundant in the EEF^{+/+} than in the EEF^{-/-} cells, suggesting that lack of *TSC2* might result in an increased amount of CD44.

Figure 3. Sorting of cultured LAM cells with anti-CD44 and anti-CD44v6 antibodies. **A**, cells sorted by side (SSC) and forward (FSC) scatter; cells within the R1 gate were selected for sorting. See Supplementary Fig. S4 for negative controls. **B**, four populations of cells defined by reaction with CD44-RPE and/or CD44v6-FITC antibodies. Cells were sorted into four different populations: CD44⁻CD44v6⁻, CD44⁺CD44v6⁻, CD44⁻CD44v6⁺, and CD44⁺CD44v6⁺. **C**, LOH for *TSC2* of genomic DNA from the four cell populations was evaluated by PCR. Chromatograms show profiles for the microsatellite marker Kg8 from LAM line 3 and D16S3395 for LAM line 6. Controls are samples from cells before sorting. Arrows, position of the missing allele. These experiments were repeated at least twice with all the 12 cell lines from the 12 patients with similar results (Table 1). **D**, permeability of CD44v6-positive cells to 7AAD; cells immunostained with the CD44v6-FITC (VFF-7) and CD44 (F10-44-2) were incubated with the vital dye 7AAD. **D**, left, graphical representation of cells positive (right, blue) or negative (left, black) for 7AAD compared with side scatter. **Middle**, graphical representation of cells positive for 7AAD and those positive for CD44-PE. PE, phycoerythrin. **Left**, graphical representation of cells positive for 7AAD and CD44v6-FITC.

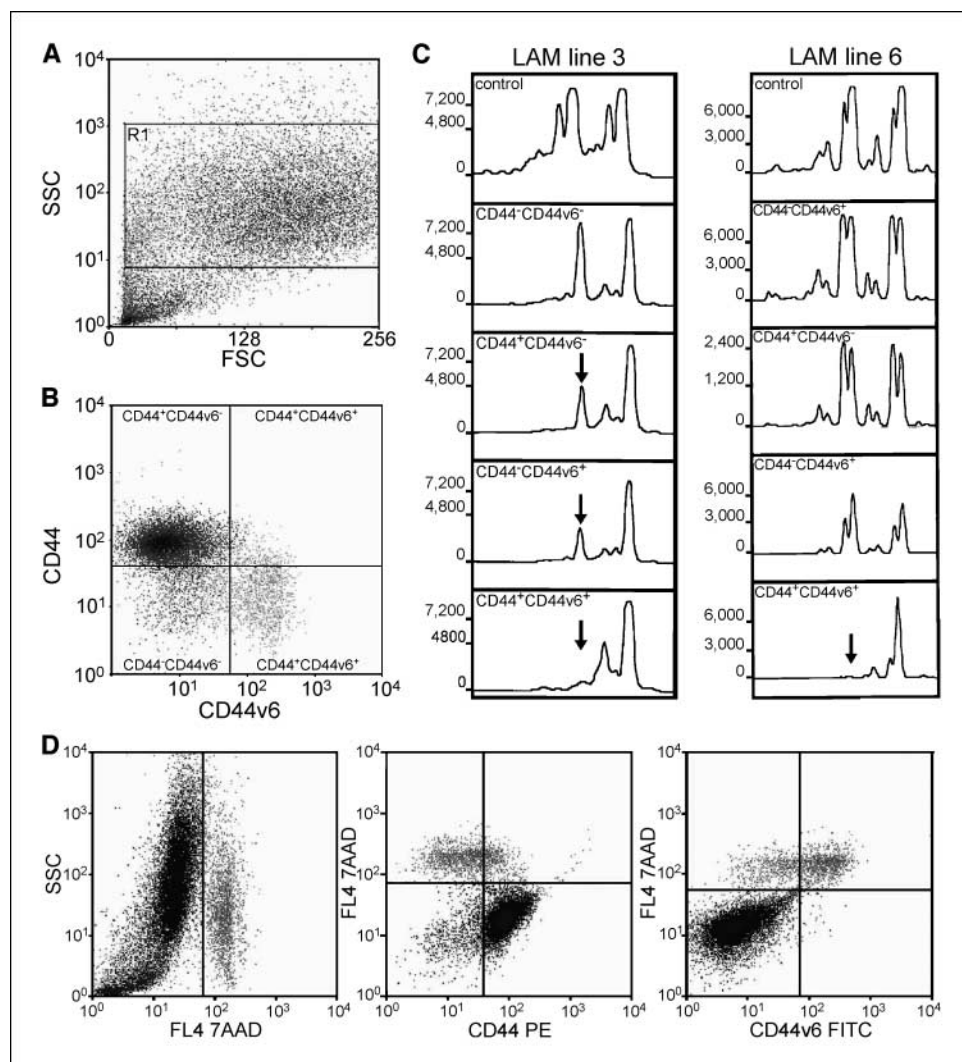


Table 1. Determination of LOH for *TSC2* in population of cells cultured from explanted lungs of patients with sporadic LAM

Cell	<i>P</i> *	CD44 ⁺ CD44v6 ⁻	CD44 ⁻ CD44v6 ⁻	CD44 ⁻ CD44v6 ⁺	CD44 ⁺ CD44v6 ⁺
LAM 1	6	R	R	LOH	LOH
LAM 2	6	LOH	R	LOH	LOH
LAM 3	6	R	R	R	LOH
LAM 4	5	LOH	R	R	LOH
LAM 5	1	LOH	R	R	LOH
LAM 6	4	R	R	R	LOH
LAM 7	3	LOH	R	R	LOH
LAM 8	4	R	R	LOH	LOH
LAM 9	5	LOH	R	LOH	LOH
LAM 10	5	R	R	LOH	LOH
LAM 11	1	LOH	R	LOH	LOH
LAM 12	1	LOH	R	LOH	LOH

Abbreviation: R; retention of heterozygosity.

*Number of times that the cells have been replated before cell sorting.

Correlation of modulators of CD44v6 splicing and CD44v6 function.

To gain insight into the regulation of CD44v6, we considered known modulators of CD44 function and its splicing (i.e., osteopontin). The concentration of osteopontin was determined in plasma of healthy volunteers ($n = 35$; mean age 52.9 ± 2.4 years) and LAM patients ($n = 40$; mean age 50.4 ± 1.7 years). Osteopontin concentration was significantly ($P < 0.001$) higher in plasma from LAM patients than in that from normal volunteers (Fig. 5). Among the 40 patients studied, eight patients had LAM and TSC. We did not observe a significant difference in the concentration of osteopontin in patients with LAM/TSC (89.8 ± 12.7 ng/mL) and sporadic LAM (72.3 ± 8.6 ng/mL). We determined the relationship of osteopontin with lung function. Osteopontin was not correlated with initial FEV1 ($P = 0.725$), initial DLCO ($P = 0.250$), rate of FEV1 decline ($P = 0.113$), and rate of decline of DLCO ($P = 0.095$). Thus, levels of osteopontin did not correlate with lung function among LAM patients. Perhaps, there was a trend toward association with rates of decline in lung function with increased osteopontin concentration. The difference between LAM patients and healthy volunteers was age and TSC independent.

We also determined the levels of CD44v6 in plasma of healthy volunteers (184.5 ± 8.9 ng/mL; $n = 35$) and LAM patients (169.4 ± 11.9 ng/mL; $n = 40$). We were not able to determine a correlation between the concentration of CD44v6 and loss of lung function (i.e., initial FEV1, initial DLCO, rate of FEV1 decline, and rate of DLCO decline).

Discussion

Cells with metastatic potential acquire distinct molecular characteristics, which determine the site(s) of metastasis. In addition, at the site of metastasis, the cells often modify their gene expression patterns, resulting in phenotypic changes that can facilitate adaptation to the new environment. To gain insight into the molecular characteristics of the LAM cells that may contribute to metastasis, we investigated whether LAM cells *in vitro* or *in vivo* synthesize CD44v6. Alternative splicing of the cell surface receptor CD44 and its overexpression have been associated with tumor metastasis and progression (12, 13, 27). Among the most

studied variants associated with tumor metastasis are CD44v6 and CD44v3 (27). CD44v6 has been associated with many cancers including squamous cell carcinoma (e.g., head and neck, esophagus, lung and skin and cervix and vulva) and adenocarcinoma [e.g., breast, Barrett's esophagus, lung, gastric, pancreas, colon/rectum, endometrium (uterine), and prostate; ref. 27]. Thus, we decided to evaluate the presence of CD44 and splice variants associated with metastasis in cells grown from patients with LAM and LAM/TSC.

LAM cells in LAM nodules exhibited only a moderate immunoreactivity for CD44, but strong immunoreactivity of other cells (e.g., vascular smooth muscle cells, bronchial epithelial cells, and hyperplastic type II pneumocytes) was noted. The limited reactivity for CD44 standard form could reflect masking of the epitope, as has been suggested for neoplastic cells. It could also represent cleavage of the CD44 standard form by metalloproteases (35) and/or other proteases acting at different sites. The stem region of CD44 contains sites for cleavage by the membrane-associated matrix metalloproteinases MMP1, MMP9, ADAM10, and ADAM17 (35). MT1-MMP and MMP-2 were found in LAM cells within the lung nodules (36), and other MMPs were overexpressed in patients with LAM. It has also been shown that regulators of MMPs are active and present in LAM lesions (37–39). We also found that the CD44 standard form was present in 90% of the cells grown from explanted lungs of LAM patients. Cells that did not react with the antibody could be those in which the receptor had been cleaved as well as truly negative (non-expressing) cells.

We found a large percentage of LAM cells within the lung nodule that reacted with the CD44v6 antibody, which strengthened our hypothesis that CD44v6 could play a role in LAM and confer metastatic potential to the LAM cells. This observation was corroborated by separation using flow cytometry of a small population of cells immunoreactive with this antibody. Cells that react with anti-CD44v6 antibodies showed LOH for *TSC2*. We also detected LOH for *TSC2* in cells in which CD44v6 was not found (CD44⁺/CD44v6⁻; Table 1), but this result was not consistent, which could be due to expression of other splice variants that may also confer metastatic potential (e.g., CD44v3).

CD44 is a protein that exists, as a result of alternative mRNA splicing, in at least 10 different variants with different functions (12). The observation of immunoreactivity for CD44v6 in cell nuclei (data not shown) might reflect its cleavage and subsequent internalization. This was shown for CD44 by presenilin/ γ -secretase at the intramembrane domain, which generated a cytoplasmic fragment that served as a transcriptional regulator (40, 41). CD44v6 seems to represent a cell surface marker expressed by LAM cells that showed LOH for *TSC2* and could help in their identification. It may also play a pivotal role in pathogenesis of the disease.

The amounts of CD44 and its splice variants at the cell surface depend, in part, on growth factor regulation of CD44 RNA splicing. Although levels of CD44 seemed to correlate with loss of *TSC2* in Fig. 4, the presence of CD44v6 did not correlate with loss of *TSC2* in

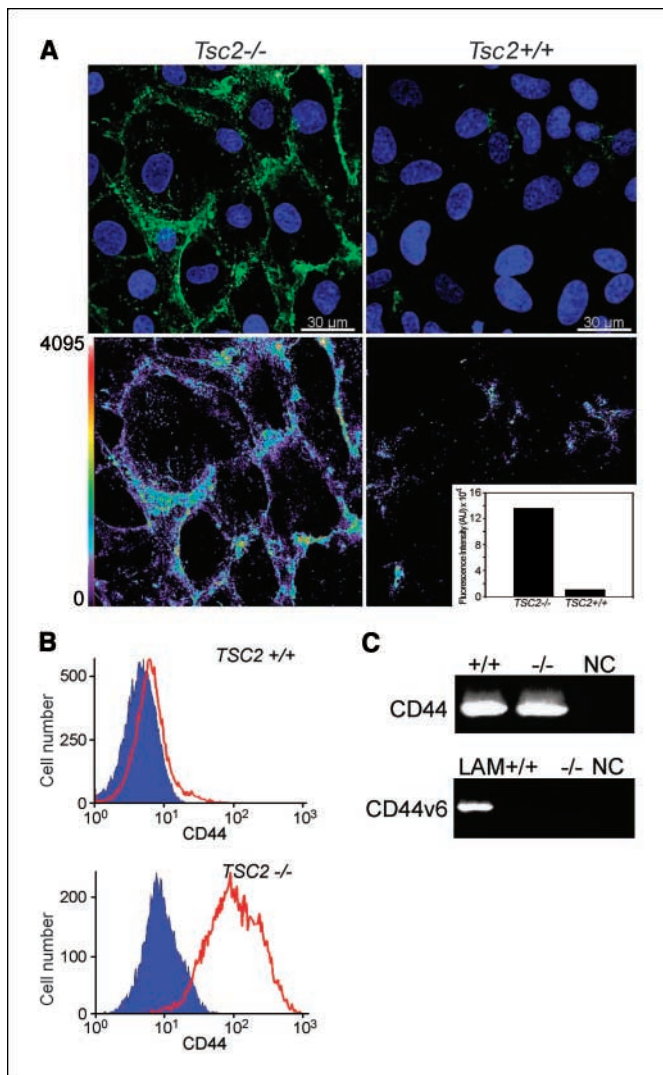


Figure 4. CD44s in Eker rat cells. *A*, CD44 and CD44v6 immunoreactivity of *Tsc2*^{-/-} and *Tsc2*^{+/+} cells. The stronger reactivity is seen in *Tsc2*^{-/-} cells than in *Tsc2*^{+/+}, which is quantified in the inset, showing that the difference is 14-fold. This experiment was repeated twice. *B*, cytometric analyses of Eker rat cells (*red*) *Tsc2*^{+/+} and *Tsc2*^{-/-} with isotype (negative) control (*blue*). *C*, the presence of CD44 mRNA in cells derived from tumors of Eker rat *Tsc2*^{+/+} and *Tsc2*^{-/-}. Detection of mRNA for CD44v6 (*bottom*) in cells derived from LAM patients (positive control) and Eker rat tumor *Tsc2*^{+/+} and *Tsc2*^{-/-}. NC, negative control (minus reverse transcriptase).

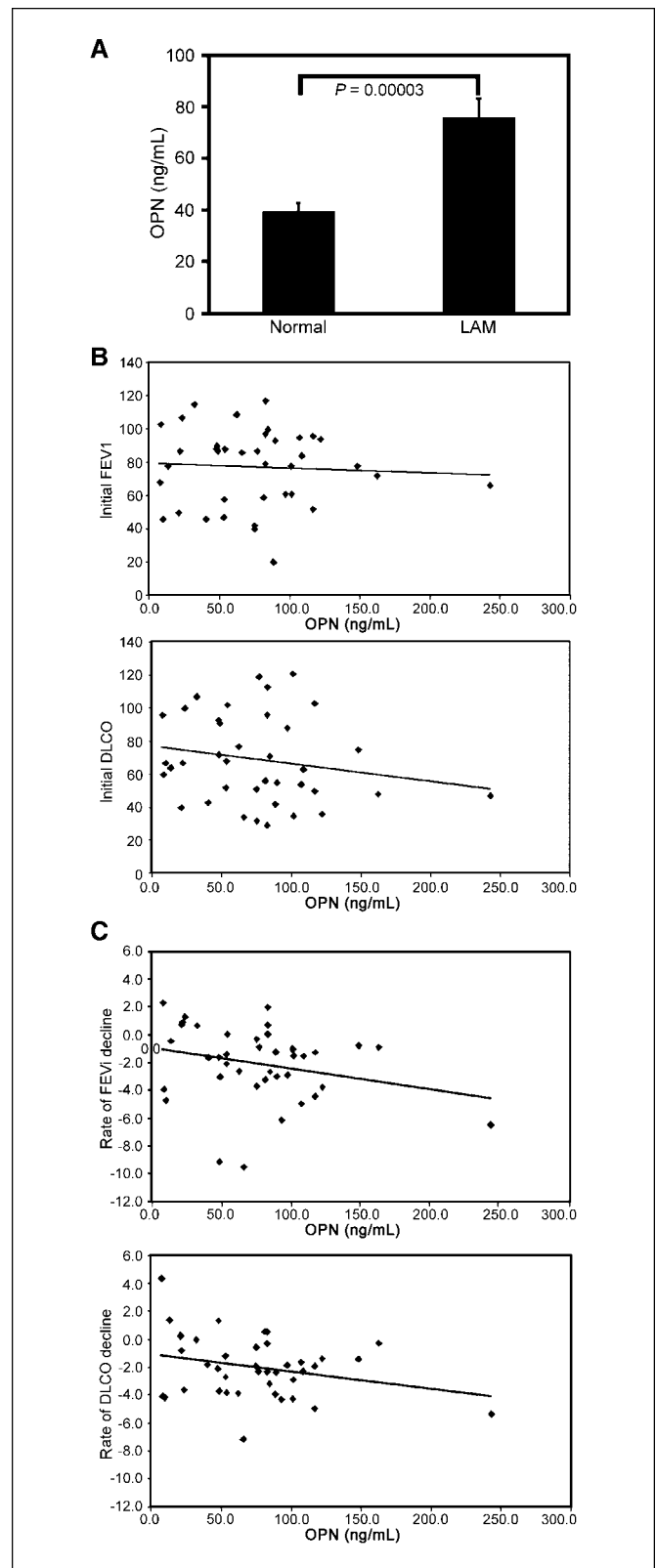


Figure 5. Concentration of osteopontin in plasma of LAM patients and normal volunteers. *A*, concentration of osteopontin (OPN) in plasma of 40 LAM patients who had not undergone lung transplantation compared with that of 35 healthy female volunteers. There was a significant difference in the levels of osteopontin, with a *P* value of 3.6×10^{-5} . *B*, correlation between the levels of osteopontin (ng/mL) with the initial FEV1 and initial DLCO. *C*, correlation between the levels of osteopontin (ng/mL) with the rate of FEV1 decline and rate of DLCO decline.

cells from the Eker rat. Thus, it seems that the LAM cells from human lung are different. CD44 splicing has been correlated with different signaling mechanisms, including those mediated by osteopontin and epidermal growth factor (13, 20, 42). In fact, the mean plasma concentration of osteopontin was higher in LAM patients than in normal volunteers (Fig. 5). Because osteopontin binds to CD44, elevated levels of osteopontin could influence cell migration (43), consistent with a potential role in disease progression. In fact, the mean plasma concentration of osteopontin was higher in LAM patients than in normal volunteers (Fig. 5).

CD44 has a single transmembrane span with a COOH-terminal cytoplasmic tail that binds the cytoskeletal protein ankyrin and members of the band 4.1 superfamily, including the tumor suppressor NF2 that encodes merlin (12) and other proteins such as ezrin. It also associates with multiple receptors (44, 45). It may be relevant that ezrin, which has been associated with tumor progression, can interact with hamartin. Thus, a dysfunctional *TSC2* as exists in LAM cells could affect the function of *TSC1* and possibly ezrin (46).

It was recently shown that the extracellular portion of CD44, including the v6 portion, sequesters Fas ligand, resulting in inhibition of apoptosis (17). Binding of Fas ligand to the CD44v6 domain was competed by anti-CD44v6. It has been shown that antibodies to CD44 can trigger apoptosis, but the mechanisms have not been clearly identified; based on the role of CD44, however, it is

possible that binding of antibody to the extracellular portion of CD44 triggers apoptosis by direct signaling events and by altering cell-to-cell and cell-to-extracellular matrix interactions.

The application of antibodies against CD44v6 in cancer diagnosis and treatment has been of interest. Binding of antibodies to CD44 has been associated with both apoptosis and cell proliferation. We observed that >80% of cells that reacted with CD44v6 antibodies were permeable to the dye 7AAD, which is presumed to indicate lack of viability. The discovery of CD44v6 in LAM cells and the potential to trigger cell death with this antibody prompt us to suggest that CD44v6 might be a therapeutic target in LAM.

Acknowledgments

Received 4/19/2007; revised 8/22/2007; accepted 8/28/2007.

Grant support: Intramural Research Program of the NIH, National Heart, Lung, and Blood Institute, and RO1 CA100907 and a Clinical Scientist Development Award from the Doris Duke Charitable Foundation (T.N. Darling).

The costs of publication of this article were defrayed in part by the payment of page charges. This article must therefore be hereby marked *advertisement* in accordance with 18 U.S.C. Section 1734 solely to indicate this fact.

We thank Dr. Martha Vaughan for helpful discussions and critical review of the manuscript; Michael Spencer for his help with the art work; Drs. Christian Combs and Daniela Malide of the microscopy core facility; Dr. Philip J. McCoy and Ann Williams of the Flow Cytometry core facility; Dr. Yoshihiko Ikeda for immunohistochemistry slides; and The LAM Foundation and The Tuberous Sclerosis Alliance for their assistance in recruiting patients for our studies.

References

- Ryu JH, Moss J, Beck GJ, et al. The NHLBI lymphangiomyomatosis registry: characteristics of 230 patients at enrollment. *Am J Respir Crit Care Med* 2006;173:105–11.
- Pacheco-Rodriguez G, Kristof AS, Stevens LA, et al. Giles F. Filley Lecture. Genetics and gene expression in lymphangiomyomatosis. *Chest* 2002;121:56–60S.
- Jóźwiak S, Schwartz RA, Janniger CK, Michalowicz R, Chmielik J. Skin lesions in children with tuberous sclerosis complex: their prevalence, natural course, and diagnostic significance. *Int J Derm* 1998;37:911–7.
- Carsillo T, Astrinidis A, Henske EP. Mutations in the tuberous sclerosis complex gene *TSC2* are a cause of sporadic pulmonary lymphangiomyomatosis. *Proc Natl Acad Sci U S A* 2000;97:6085–90.
- Wullschlegel S, Loewith R, Hall MN. TOR signaling in growth and metabolism. *Cell* 2006;124:471–84.
- Goncharova EA, Goncharov DA, Eszterhas A, et al. Tuberin regulates p70 S6 kinase activation and ribosomal protein S6 phosphorylation. A role for the *TSC2* tumor suppressor gene in pulmonary lymphangiomyomatosis (LAM). *J Biol Chem* 2002;277:30958–67.
- Ferrans VJ, Yu ZX, Nelson WK, et al. Lymphangiomyomatosis (LAM): a review of clinical and morphological features. *J Nippon Med Sch* 2000;67:311–29.
- Crooks DM, Pacheco-Rodriguez G, DeCastro RM, et al. Molecular and genetic analysis of disseminated neoplastic cells in lymphangiomyomatosis. *Proc Natl Acad Sci U S A* 2004;101:17462–7.
- Henske EP. Metastasis of benign tumor cells in tuberous sclerosis complex. *Genes Chromosomes Cancer* 2003;38:376–81.
- Karbowiczek M, Yu J, Henske EP. Renal angiomyolipomas from patients with sporadic lymphangiomyomatosis contain both neoplastic and non-neoplastic vascular structures. *Am J Pathol* 2003;162:491–500.
- Bittmann I, Rolf B, Amann G, Lohrs U. Recurrence of lymphangiomyomatosis after single lung transplantation: new insights into pathogenesis. *Hum Pathol* 2003;34:95–8.
- Ponta H, Sherman L, Herrlich PA. CD44: from adhesion molecules to signalling regulators. *Nat Rev Mol Cell Biol* 2003;4:33–45.
- Marhaba R, Zoller M. CD44 in cancer progression: adhesion, migration and growth regulation. *J Mol Histol* 2004;35:211–31.
- Gunthert U, Hofmann M, Rudy W, et al. A new variant of glycoprotein CD44 confers metastatic potential to rat carcinoma cells. *Cell* 1991;65:13–24.
- Weg-Remers S, Ponta H, Herrlich P, König H. Regulation of alternative pre-mRNA splicing by the ERK MAP-kinase pathway. *EMBO J* 2001;20:4194–203.
- Bajorath J. Molecular organization, structural features, and ligand binding characteristics of CD44, a highly variable cell surface glycoprotein with multiple functions. *Proteins* 2000;39:103–11.
- Mielgo A, van Driel M, Bloem A, Landmann L, Gunthert U. A novel antiapoptotic mechanism based on interference of Fas signaling by CD44 variant isoforms. *Cell Death Differ* 2006;13:465–77.
- Okamoto I, Kawano Y, Murakami D, et al. Proteolytic release of CD44 intracellular domain and its role in the CD44 signaling pathway. *J Cell Biol* 2001;155:755–62.
- Recio JA, Merlino G. Hepatocyte growth factor/scatter factor induces feedback up-regulation of CD44v6 in melanoma cells through Egr-1. *Cancer Res* 2003;63:1576–82.
- Gao C, Guo H, Downey L, et al. Osteopontin-dependent CD44v6 expression and cell adhesion in HepG2 cells. *Carcinogenesis* 2003;24:1871–8.
- Senger DR, Perruzzi CA, Papadopoulos-Sergiou A, Van de Water L. Adhesive properties of osteopontin: regulation by a naturally occurring thrombin-cleavage in close proximity to the GRGDS cell-binding domain. *Mol Biol Cell* 1994;5:565–74.
- Agnihotri R, Crawford HC, Haro H, et al. Osteopontin, a novel substrate for matrix metalloproteinase-3 (stromelysin-1) and matrix metalloproteinase-7 (matrilysin). *J Biol Chem* 2001;276:28261–7.
- Katagiri YU, Sleeman J, Fujii H, et al. CD44 variants but not CD44s cooperate with β 1-containing integrins to permit cells to bind to osteopontin independently of arginine-glycine-aspartic acid, thereby stimulating cell motility and chemotaxis. *Cancer Res* 1999;59:219–26.
- Rangaswami H, Bulbule A, Kundu GC. Osteopontin: role in cell signaling and cancer progression. *Trends Cell Biol* 2006;16:79–87.
- Achen MG, McColl BK, Stacker SA. Focus on lymphangiogenesis in tumor metastasis. *Cancer Cell* 2005;7:121–7.
- Chambers AF, Groom AC, MacDonald IC. Dissemination and growth of cancer cells in metastatic sites. *Nat Rev Cancer* 2002;2:563–72.
- Heider KH, Kuthan H, Stehle G, Munzert G. CD44v6: a target for antibody-based cancer therapy. *Cancer Immunol Immunother* 2004;53:567–79.
- Pittenger MF, Mackay AM, Beck SC, et al. Multipotential differentiation of adult human mesenchymal stem cells. *Science* 1999;284:143–7.
- Hudson DL, Sleeman J, Watt FM. CD44 is the major peanut lectin-binding glycoprotein of human epidermal keratinocytes and plays a role in intercellular adhesion. *J Cell Sci* 1995;108:1959–70.
- Kasper M, Gunthert U, Dall P, et al. Distinct expression patterns of CD44 isoforms during human lung development and in pulmonary fibrosis. *Am J Respir Cell Mol Biol* 1995;13:648–56.
- Kahn HJ, Bailey D, Marks A. Monoclonal antibody D2-40, a new marker of lymphatic endothelium, reacts with Kaposi's sarcoma and a subset of angiosarcomas. *Mod Pathol* 2002;15:434–40.
- Kleymenova E, Ibraghimov-Beskrovnaya O, Kugoh H, et al. Tuberin-dependent membrane localization of polycystin-1: a functional link between polycystic kidney disease and the *TSC2* tumor suppressor gene. *Mol Cell* 2001;7:823–32.
- Schmid I, Uittenbogaart CH, Keld B, Giorgi JV. A rapid method for measuring apoptosis and dual-color immunofluorescence by single laser flow cytometry. *J Immunol Methods* 1994;170:145–57.
- Soucek T, Yeung RS, Hengstschiager M. Inactivation of the cyclin-dependent kinase inhibitor p27 upon loss of the tuberous sclerosis complex gene-2. *Proc Natl Acad Sci U S A* 1998;95:15653–8.

35. Nagano O, Saya H. Mechanism and biological significance of CD44 cleavage. *Cancer Sci* 2004;95:930-5.
36. Matsui K, Takeda K, Yu ZX, et al. Role for activation of matrix metalloproteinases in the pathogenesis of pulmonary lymphangioleiomyomatosis. *Arch Pathol Lab Med* 2000;124:267-75.
37. Zhe X, Yang Y, Jakkaraju S, Schuger L. Tissue inhibitor of metalloproteinase-3 downregulation in lymphangioleiomyomatosis: potential consequence of abnormal serum response factor expression. *Am J Respir Cell Mol Biol* 2003;28:504-11.
38. Zhe X, Yang Y, Schuger L. Imbalanced plasminogen system in lymphangioleiomyomatosis: potential role of serum response factor. *Am J Respir Cell Mol Biol* 2005; 32:28-34.
39. Ferri N, Carragher NO, Raines EW. Role of discoidin domain receptors 1 and 2 in human smooth muscle cell-mediated collagen remodeling; potential implications in atherosclerosis and lymphangioleiomyomatosis. *Am J Pathol* 2004;164:1575-85.
40. Lammich S, Okochi M, Takeda M, et al. Presenilin-dependent intramembrane proteolysis of CD44 leads to the liberation of its intracellular domain and the secretion of an A β -like peptide. *J Biol Chem* 2002;277: 44754-9.
41. Murakami D, Okamoto I, Nagano O, et al. Presenilin-dependent γ -secretase activity mediates the intramembranous cleavage of CD44. *Oncogene* 2003;22:1511-6.
42. Hebbard L, Steffen A, Zawadzki V, et al. CD44 expression and regulation during mammary gland development and function. *J Cell Sci* 2000;113: 2619-30.
43. Zhu B, Suzuki K, Goldberg HA, et al. Osteopontin modulates CD44-dependent chemotaxis of peritoneal macrophages through G-protein-coupled receptors: evidence of a role for an intracellular form of osteopontin. *J Cell Physiol* 2004;198:155-67.
44. Corso S, Comoglio PM, Giordano S. Cancer therapy: can the challenge be MET? *Trends Mol Med* 2005;11: 284-92.
45. Orian-Rousseau V, Chen L, Sleeman JP, Herrlich P, Ponta H. CD44 is required for two consecutive steps in HGF/c-Met signaling. *Genes Dev* 2002;16: 3074-86.
46. Lamb RF, Roy C, Diefenbach TJ, et al. The TSC1 tumour suppressor hamartin regulates cell adhesion through ERM proteins and the GTPase Rho. *Nat Cell Biol* 2000;2:281-7.